NASA Contractor Report 191519
ICASE Report No. 93-58

ICASE

20 Years of Excellence

ON THE RECEPTIVITY PROBLEM FOR 0(1) WAVELENGTH GÖRTLER VORTICES

Andrew P. Bassom
Philip Hall

NASA Contract No. NAS1-19480
August 1993

Institute for Computer Applications in Science and Engineering
NASA Langley Research Center
Hampton, Virginia 23681-0001

Operated by the Universities Space Research Association

National Aeronautics and
Space Administration

Langley Research Center
Hampton, Virginia 23681-0001

ICASE Fluid Mechanics

Due to increasing research being conducted at ICASE in the field of fluid mechanics, future ICASE reports in this area of research will be printed with a green cover. Applied and numerical mathematics reports will have the familiar blue cover, while computer science reports will have yellow covers. In all other aspects the reports will remain the same; in particular, they will continue to be submitted to the appropriate journals or conferences for formal publication.

THE RECEPTIVITY PROBLEM FOR O(1) WAVELENGTH GÖRTLER VORTICES

Andrew P. Bassom[1]
Department of Mathematics
University of Exeter
North Park Road
Exeter, Devon EX4 4QE
UNITED KINGDOM

and

Philip Hall[1]
Department of Mathematics
University of Manchester
Oxford Road
Manchester. M13 9PL
UNITED KINGDOM

ABSTRACT

In this paper we make an investigation of the receptivity of boundary layer flows to Görtler vortex modes. A study by Denier, Hall & Seddougui (1991) of the generation of vortices by wall roughness elements concluded that such elements are extremely poor as mechanisms to stimulate short wavelength modes. That work also examined the equivalent problem pertaining to O(1) wavelength modes but that analysis was in error. We re-examine this problem here and demonstrate how the form of the wall roughness is crucial in determining the vortex stability characteristics downstream of the roughness. In particular we investigate the cases of both isolated and distributed forcing functions and show that in general a distributed function is much more important in generating vortices than are either isolated roughness or free–stream disturbances.

[1]This research was supported by the National Aeronautics and Space Administration under NASA Contract No. NAS1-19480 while the authors were in residence at the Institute for Computer Applications in Science and Engineering (ICASE), NASA Langley Research Center, Hampton, VA 23681.

1. Introduction

Until quite recently little was known about the important problem of the receptivity of boundary layers to Görtler vortices. Perhaps the first work in this direction was performed by Hall (1990) who was concerned with the receptivity question in the case of vortices excited by free–stream disturbances. That paper also reviews the various stages of growth of Görtler vortices within boundary layers and the reader is referred to that article for an extended discussion of the linear and nonlinear characteristics of Görtler modes.

The receptivity work of Hall (1990) used a linearised analysis and this was extended by Denier, Hall & Seddougui (1991) (hereafter referred to as DHS) in order to account for the processes by which Görtler vortices may be stimulated by wall roughness elements. DHS considered both isolated and distributed roughness patches and they calculated coupling coefficients which indicate how the amplitude of the forcing function is related to the induced vortex size. For small vortex wavelength the coupling coefficient is exponentially small and so it was concluded that this type of mode is unlikely to be directly excited by wall roughness.

This finding concerning the receptivity of boundary layers to high wavenumber vortices was deduced using an analytical technique in which the flow structure was described by WKB type expansions. However, in general a numerical method is required in order to investigate the properties of O(1) wavenumber Görtler vortices generated by roughness. Laplace transform solutions of the governing equations were used by DHS in order to calculate the structure of the vortices at small distances downstream of the roughness region. This structure could then be used as initial conditions for the numerical marching of the relevant equations in order to obtain the flow properties at O(1) distances from the roughness. These initial conditions assume the form of similarity solutions and the disturbance structure as predicted by DHS implies that close to the roughness the vortex is effectively confined to a very thin layer adjacent to the bounding surface of the flow.

The type of analysis outlined in DHS was also used by Hall & Morris (1992) in the context of describing how vortices develop in the flow over a heated flat plate when these modes are triggered either by localised or distributed wall roughness or by non–uniform wall heating. Both these papers concluded that for O(1) wavelength modes a vortex field grows within a wedge at a finite distance downstream of the non–uniformity in the flow.

Subsequent investigations of the receptivity of Görtler vortices have suggested that the work of DHS for O(1) wavenumber modes is erroneous for two reasons. First, the inversion of the Laplace transform solutions derived in DHS are technically more involved than as was presented. This in turn has implications for the similarity solution structures and we show below that the required structure is not confined in the thin wall layer predicted by DHS. Therefore the numerical solutions obtained by DHS by integrating the full equations were initiated with incorrect disturbance profiles and so the aim of the current work is to

reconsider this O(1) wavenumber study. This allows us to illustrate how the analysis and conclusions of DHS need to be amended. First we concentrate on the problem with an isolated roughness element and then demonstrate how useful deductions concerning the distributed situation may be obtained.

To begin we shall give a brief derivation of the pertinent equations, fuller details of which may be found in DHS. Consider the flow of a viscous fluid over a wall of variable curvature. If U_∞ is a typical flow velocity far from the wall, ν is the kinematic viscosity of the fluid and L is a typical lengthscale over which the wall curvature varies then we define a Reynolds number Re by

$$Re = U_\infty L/\nu, \tag{1.1}$$

and we suppose that with respect to Cartesian axes x^*, y^*, z^* the wall is defined by

$$y^* = L\left[Re^{-\frac{1}{2}} g(x^*/L) + \Delta Re^{-\frac{1}{2}} f\left(x^*/L, Re^{\frac{1}{2}} z^*/L\right)\right], \tag{1.2}$$

where Δ is a small constant. Variables (x, y, z) are defined according to

$$(x, y, z) = (x^*, Re^{\frac{1}{2}} y^*, Re^{\frac{1}{2}} z^*)/L, \tag{1.3a}$$

and the corresponding velocity vector is supposed to be given by

$$(u^+, v^+, w^+) = (u^*, Re^{\frac{1}{2}} v^*, Re^{\frac{1}{2}} w^*)/U_\infty. \tag{1.3b}$$

Attention is confined to the limit $Re \to \infty$ and then

$$p^+ = \bar{p}(x) + \Delta Re^{-\frac{1}{2}} \tilde{p}(x, y, z) + O(\Delta^2), \qquad (u^+, v^+, w^+) = (\bar{u}, \bar{v}, 0) + \Delta(\tilde{u}, \tilde{v}, \tilde{w}) + O(\Delta^2), \tag{1.4a, b}$$

where p^+ is the fluid pressure scaled on ρU_∞^2 with ρ the fluid density. The basic flow velocities $\bar{u}, \bar{v}$ are functions of x and y alone whilst $\tilde{u}, \tilde{v}, \tilde{w}, \tilde{p}$ depend on all three spatial co-ordinates. Expressions $(1.4a, b)$ are substituted into the linearised Navier–Stokes and continuity equations and the resulting forms need to be solved subject to no–slip conditions on the wall $y = g$ and need also match to the free stream fluid velocity as $y \to \infty$. As in DHS we shall restrict our analysis to Blasius flow as a specific example although it is straightforward to generalise the work to other basic boundary layers.

It is convenient to apply a suitable Prandtl transformation to the linearised disturbance equations to give

$$\tilde{u}_x + \tilde{v}_y + \tilde{w}_z = 0, \tag{1.5a}$$

$$\bar{u}\tilde{u}_x + \bar{v}\tilde{u}_y + \tilde{v}\bar{u}_y + \tilde{u}\bar{u}_x = \tilde{u}_{yy} + \tilde{u}_{zz}, \tag{1.5b}$$

$$\bar{u}\tilde{v}_x + \bar{v}\tilde{v}_y + \tilde{u}\bar{v}_x + \tilde{v}\bar{v}_y + G\chi(x)\bar{u}\tilde{u} = -\tilde{p}_y + \tilde{v}_{yy} + \tilde{v}_{zz}, \tag{1.5c}$$

$$\bar{u}\tilde{w}_x + \bar{v}\tilde{w}_y = -\tilde{p}_z + \tilde{w}_{yy} + \tilde{w}_{zz}, \tag{1.5d}$$

$$\tilde{u} = -f\bar{u}_y, \quad \tilde{v} = \tilde{w} = 0 \qquad \text{on} \qquad y = 0, \tag{1.5e}$$

$$\tilde{u}, \tilde{v}, \tilde{w} \to 0 \qquad \text{as} \qquad y \to \infty, \tag{1.5f}$$

whilst the basic flow quantities satisfy

$$\bar{u}_x + \bar{v}_y = 0, \qquad \bar{u}\bar{u}_x + \bar{v}\bar{u}_y = -\bar{p}_x + \bar{u}_{yy},$$

$$\bar{u} = \bar{v} = 0 \qquad \text{on} \quad y = 0; \qquad \bar{u} \to 1 \qquad \text{as} \quad y \to \infty.$$

In equation (1.5c) the quantity $2(d^2g/dx^2)$ has been replaced by $G\chi(x)$ where χ and G are referred to as the wall curvature and Görtler number respectively. It is convenient to assume that the function $f(x,z)$ (which determines the geometry of the roughness on the wall) may be written as $f = \tilde{f}(x)\tilde{q}(z)$ and then equations (1.5) may be Fourier transformed in z. If $u, v, \ldots$ denote the Fourier transforms of $\tilde{u}, \tilde{v}, \ldots$ etc. then it is convenient to eliminate w and p from the transformed versions of (1.5). If k denotes the transform variable then we obtain

$$\bar{u}u_x + \bar{v}u_y + v\bar{u}_y + u\bar{u}_x = u_{yy} - k^2u, \tag{1.6a}$$

$$\begin{aligned}\left\{\bar{u}_{xyy} + k^4 + k^2\bar{v}_y\right\}v + \bar{v}_x u_{yy} + \left\{\bar{u}_{xyy} + k^2\bar{v}_x + k^2\chi G\bar{u}\right\}u \\ + \left\{\bar{u}_{yy} - \bar{u}\partial^2/\partial y^2 + k^2\bar{u}\right\}v_x + 2\left\{\bar{u}_{xy} + \bar{u}_x\partial/\partial y\right\}u_x \\ + v_{yyyy} - \bar{v}v_{yyy} - \left\{\bar{v}_y + 2k^2\right\}v_{yy} + \left\{\bar{u}_{xy} + k^2\bar{v}\right\}v_y = 0,\end{aligned} \tag{1.6b}$$

linking u and v whilst w and p may be then deduced from the transformed versions of (1.5a, d)

$$u_x + v_y + ikw = 0, \tag{1.6c}$$

$$\bar{u}w_x + \bar{v}w_y = -ikp + w_{yy} - k^2w, \tag{1.6d}$$

should these quantities be desired. On defining $F(x) = \bar{u}_y(x,0)\tilde{f}(x)$ it is found that equations (1.6) need to be solved subject to

$$u = q(k)F(x), \quad v = w = 0, \qquad \text{on} \qquad y = 0, \tag{1.6e}$$

$$u, v, w \longrightarrow 0 \qquad \text{as} \qquad y \longrightarrow \infty. \tag{1.6f}$$

DHS showed that wall roughness is inefficient in stimulating small wavelength Görtler vortices and so here we shall be concerned solely with the case when the forced vortex wavelength is comparable with the boundary layer thickness. For all the work undertaken it transpires that the factor $q(k)$ is merely a multiplicative constant so henceforth we shall take $q(k) \equiv 1$ which corresponds to a delta–function shaped hump in the spanwise direction. Corresponding results for other spanwise distributions may be deduced easily.

The remainder of this paper is divided as follows. In §2 we determine solutions appropriate to the case when $F(x)$ varies on a relatively fast lengthscale. DHS demonstrated that, at least in theory, the asymptotic forms of these solutions can be used as the (necessarily unique) initial conditions for marching the full linearised equations $(1.6a, b)$ in the streamwise direction x. These initial conditions are studied in §3 and the subsequent numerical solutions addressed in §4. We conclude with a brief discussion of the implications of this study.

2. Vortices induced by short scale roughness elements

We now examine solutions of $(1.6a, b)$ when the forcing function $F(x)$ varies on a fast, say $O(\varepsilon)$, lengthscale. Suppose that the forcing begins at $x = \bar{x}$ and define

$$X = (x - \bar{x})/\varepsilon \qquad \text{and} \qquad F(x) = F^*(X). \tag{2.1}$$

DHS pointed out that we may take $\bar{x} = \frac{1}{2}$ without loss of generality so that the original lengthscale L has been fixed in terms of the distance from the leading edge to the position where the forcing begins. In the neighbourhood of $\bar{x} = \frac{1}{2}$ then convective and vertical diffusion effects are comparable in a region of depth $O(\varepsilon^{\frac{1}{3}})$ and the wall forcing implies that u will be O(1) there. If we define

$$\xi = y/\varepsilon^{\frac{1}{3}}$$

then for $\xi = O(1)$ the disturbance quantities develop as

$$(u, v, w, p) = \left(u_0(X, \xi), \varepsilon^{-\frac{2}{3}} v_0(X, \xi), \varepsilon^{-1} w_0(X, \xi), \varepsilon^{-\frac{5}{3}} p_0(X, \xi)\right) + \ldots, \tag{2.2a}$$

whilst

$$(\bar{u}, \bar{v}) = \left(\varepsilon^{\frac{1}{3}} \lambda \xi, \varepsilon^{\frac{2}{3}} \mu \xi^2\right) + \ldots. \tag{2.2b}$$

If the governing equations $(1.6a, b)$ are Laplace–transformed with respect to X and solutions of the forms $(2.2a)$ sought then DHS demonstrated that the transformed functions $\bar{u}_0, \bar{v}_0$ are given by

$$\begin{aligned}\bar{u}_0(s, \xi) =& \frac{\bar{F}(s)}{\mathrm{Ai}(0)} \mathrm{Ai}\left[(\lambda s)^{\frac{1}{3}} \xi\right] \\ &+ \lambda \mathrm{Ai}\left[(\lambda s)^{\frac{1}{3}} \xi\right] \int_0^{\xi} \frac{dp}{\left[\mathrm{Ai}\left((\lambda s)^{\frac{1}{3}} p\right)\right]^2} \left\{\int_{\infty}^{p} \bar{v}_0(s, q) \mathrm{Ai}\left((\lambda s)^{\frac{1}{3}} q\right) dq\right\},\end{aligned} \tag{2.3a}$$

$$\bar{v}_0(s, \xi) = -3\lambda^{\frac{1}{3}} s^{\frac{4}{3}} \bar{F}(s) \left[(s\lambda)^{-\frac{2}{3}} \left\{\mathrm{Ai}'\left[(\lambda s)^{\frac{1}{3}} \xi\right] - \mathrm{Ai}'(0)\right\} + \xi \int_{\xi}^{\infty} \mathrm{Ai}\left[(\lambda s)^{\frac{1}{3}} q\right] dq\right], \tag{2.3b}$$

where s denotes the transform variable and Ai is the usual Airy function. Furthermore, by considering these expressions as $\xi \to \infty$, it was shown that the flow in this wall layer induces a motion in the zone $y = O(1)$ and there

$$u = U_0 \varepsilon^{\frac{1}{3}} + \ldots, \qquad v = V_0 \varepsilon^{-\frac{2}{3}} + \ldots, \tag{2.4a}$$

where $\bar{U}_0, \bar{V}_0$, the transforms of U_0 and V_0, are given by

$$\bar{U}_0 = \frac{3\bar{F}(s)\bar{u}'}{\bar{u}} (s\lambda)^{-\frac{1}{3}} \operatorname{Ai}'(0) q^*(y,k) + \ldots, \qquad \bar{V}_0 = -3\bar{F}(s) s^{\frac{2}{3}} \lambda^{-\frac{1}{3}} \operatorname{Ai}'(0) q^*(y,k) + \ldots, \tag{2.4b}$$

with q^* satisfying the stationary Rayleigh problem

$$\bar{u}\left(\partial_y^2 - k^2\right) q^* - \bar{u}'' q^* = 0, \qquad q^*(0) = 1, \quad q^*(\infty) = 0. \tag{2.4c}$$

DHS restricted their attention to the case when $F^* = \delta(X)$ and showed that this choice leads to a solution in which

$$u_0 \sim \frac{1}{X} \tilde{\bar{u}}_0 \left(\xi / X^{\frac{1}{3}}\right), \qquad v_0 \sim \frac{1}{X^{\frac{5}{3}}} \tilde{\bar{v}}_0 \left(\xi / X^{\frac{1}{3}}\right). \tag{2.4d}$$

This in turn suggests a form of similarity solution as appropriate initial conditions for a numerical solution of the system $(1.6a, b)$ to O(1) distances downstream of the delta–function shaped hump. However, DHS were unable to obtain similarity solutions of the type assumed in $(2.4d)$ and so they proposed an alternative form which had the unusual feature of predicting that the disturbed flow remains confined to a thin wall layer even at O(1) distances from the roughness. We demonstrate that this conclusion is incorrect (see §3) but first we examine the inversion of expressions $(2.3a, b)$ for an illustrative selection of roughness functions $F^*(X)$.

Since the transformed quantities $\bar{u}_0$, $\bar{v}_0$ involve Airy functions of argument proportional to $s^{\frac{1}{3}}$ it is clear that in order to obtained the inverted forms u_0, v_0 it is essential to cut the complex s-plane in an appropriate manner. It is a standard result of transform theory that if $\bar{Q}(s)$ is the Laplace transform of any suitably well behaved function $Q(X)$ then

$$Q(X) = \frac{1}{2\pi i} \int_{c-i\infty}^{c+i\infty} e^{sX} \bar{Q}(s) ds,$$

where the line of integration passes to the right of any singularities in $\bar{Q}(s)$. If we cut the s-plane along the $\arg(s) = \pi$ ray then we can invert $\bar{Q}(s)$ by integrating around the classical 'key-hole' shaped contour sketched in Figure 1 and which is composed of a large semi-circular arc of radius R and linear portions $\mathcal{L}_1, \mathcal{L}_2, \mathcal{L}_3, \mathcal{L}_4$ and $\mathcal{L}_5$. The first two of the straight line contours are located just above and below the branch cut and a small circle $\mathcal{C}$, radius δ, which has centre $s = 0$. For all physically realistic roughness shapes it is

straightforward to verify that, assuming the semi-circular arc is chosen so as to avoid any singularities in $\bar{Q}(s)$, then as $R \to \infty$ the integrals over the straight lines $\mathcal{L}_3, \mathcal{L}_4$ and the semi-circle $\longrightarrow 0$ and the inverse of $\bar{Q}(s)$ follows once $\delta \to 0$.

We now demonstrate how contributions from $\mathcal{L}_1$, $\mathcal{L}_2$, $\mathcal{C}$ and any poles can play contrasting roles as the forcing function $F^*(X)$ is varied. Interest is restricted to the case $X \longrightarrow \infty$ for this limit indicates the appropriate initial conditions for a numerical solution of equations $(1.6a, b)$ in order to obtain the vortex characteristics for $x = O(1)$.

2.1. The delta function $F^*(X) = \delta(X)$.

Now $\bar{F}(s) = 1$ and so $\bar{u}_0$ and $\bar{v}_0$ have no poles in the s-plane. In addition the contribution from $\mathcal{C} \longrightarrow 0$ as its radius shrinks to zero so that the dominant part of the solution must arise from the integrals along $\mathcal{L}_1$ and $\mathcal{L}_2$. If we define

$$-sX = \theta^3, \qquad \xi = X^{\frac{1}{3}}\eta/\lambda^{\frac{1}{3}}, \tag{2.5}$$

then

$$v_0 = \frac{9\lambda^{-\frac{1}{3}}}{2\pi i X^{\frac{5}{3}}} N, \tag{2.6a}$$

where

$$N(\eta) = \int_0^\infty \theta^4 \exp(-\theta^3)\Big[e^{\frac{2i\pi}{3}} \operatorname{Ai}'\left(\theta\eta e^{\frac{i\pi}{3}}\right) - e^{-\frac{2i\pi}{3}} \operatorname{Ai}'\left(\theta\eta e^{-\frac{i\pi}{3}}\right) - i\sqrt{3}\operatorname{Ai}'(0) + \theta^2\eta \int_\eta^\infty \left(e^{-\frac{2i\pi}{3}} \operatorname{Ai}\left(\theta t e^{\frac{i\pi}{3}}\right) - e^{\frac{2i\pi}{3}} \operatorname{Ai}\left(\theta t e^{-\frac{i\pi}{3}}\right)\right) dt\Big] d\theta.$$

Elementary analysis demonstrates that

$$N'''' + \tfrac{1}{3}\eta^2 N''' + \tfrac{7}{3}\eta N'' = 0, \tag{2.6b}$$

with

$$N(0) = N'(0) = 0, \quad N''(0) = \frac{i\operatorname{Ai}(0)}{\sqrt{3}}\Gamma(\tfrac{7}{3}), \quad N'''(0) = \frac{i\operatorname{Ai}'(0)}{\sqrt{3}}\Gamma(\tfrac{8}{3}), \tag{2.6c}$$

and where $'$ denotes a derivative with respect with to η. It is possible to express N in terms of the Whittaker function $W_{\kappa,\nu}$ defined in Abramowitz & Stegun (1965) so that

$$N'' = \frac{4i}{9^{\frac{11}{12}}} \operatorname{Ai}(0)\Gamma(-\tfrac{4}{3})\eta^{-1} \exp\left(-\tfrac{1}{18}\eta^3\right) W_{2,\frac{1}{6}}\left(\tfrac{1}{9}\eta^3\right). \tag{2.7}$$

A study of the inversion of $(2.3a)$ leads to the solution

$$u_0 = -\frac{9}{2i\pi X}\left[-\frac{i}{9\sqrt{3}}\left(7\operatorname{Ai}(0) + \frac{3\operatorname{Ai}'(0)}{\operatorname{Ai}(0)}\right)\Gamma(\tfrac{4}{3})\eta \exp\left(-\tfrac{1}{9}\eta^3\right) + \tfrac{1}{6}\eta N'' - \tfrac{1}{3}N' + \tfrac{5}{18}\eta^2 N - \eta \exp\left(-\tfrac{1}{9}\eta^3\right) \int_0^\eta \left(\tfrac{7}{9} + \tfrac{5}{54}t^3\right) N(t) \exp\left(\tfrac{1}{9}t^3\right) dt\right], \tag{2.8}$$

and the solutions (2.6a), (2.8) together give the large X solution (2.2a). Although they are not required in this study, the relevant forms of the spanwise velocity and pressure disturbance components, w_0 and p_0, may now be retrieved from (1.6c, d).

2.2. The Heaviside function $F^*(X) = H(X)$.

In this case $\bar{F}(s) = 1/s$ and the inversion of $\bar{u}_0(s, \xi)$ no longer has a negligible contribution from the small circle $\mathcal{C}$ as $\delta \to 0$. If the substitutions (2.5) are made it is a straightforward but lengthy task to deduce that as $X \to \infty$

$$v_0 = -\frac{9^{\frac{1}{3}}\lambda^{-\frac{1}{3}}}{4\pi^2 X^{\frac{2}{3}}}\Gamma(-\tfrac{1}{3})\Gamma(\tfrac{2}{3})\hat{N}(\eta), \tag{2.9a}$$

where

$$\hat{N}'''' + \tfrac{1}{3}\eta^2\hat{N}''' + \tfrac{4}{3}\eta\hat{N}'' = 0: \quad \hat{N}(0) = \hat{N}'(0) = 0, \quad \hat{N} \to 1 \quad \text{as} \quad \eta \to \infty, \tag{2.9b}$$

or, equivalently,

$$v_0 = -\frac{3\sqrt{3}\lambda^{-\frac{1}{3}}}{2\pi X^{\frac{2}{3}}}\int_0^\eta \left(\frac{\eta}{t} - 1\right)\exp\left(-\tfrac{1}{18}t^3\right) W_{1,\frac{1}{6}}\left(\tfrac{1}{9}t^3\right) dt. \tag{2.9c}$$

In turn, inversion of (2.3a) leads to

$$\begin{aligned} u_0 = &\frac{9^{\frac{1}{6}}}{\Gamma(\frac{1}{3})}\left\{\int_\infty^0 \exp\left(-\tfrac{1}{9}p^3\right)\left[\int_0^p v_0(q)\exp\left(\tfrac{1}{9}q^3\right) dq\right] dp - 1\right\}\int_\infty^\eta \exp\left(-\tfrac{1}{9}t^3\right) dt \\ &+ \int_\infty^\eta \exp\left(-\tfrac{1}{9}p^3\right)\left[\int_0^p v_0(q)\exp\left(\tfrac{1}{9}q^3\right) dq\right] dp. \end{aligned} \tag{2.9d}$$

2.3. A distributed roughness element.

In order to illustrate the effect of a distributed as opposed to an isolated roughness patch we now consider a forcing function given by

$$F^*(X) = \sin X. \tag{2.10}$$

In this case $\bar{F}(s) = 1/(1 + s^2)$ and this introduces simple poles into the Laplace inversion integrals required in order to deduce u_0 and v_0. For this particular choice of forcing function $\bar{F}(s) \to 1$ as $s \to 0$ and thus the contributions to $u_0(X, \xi)$, $v_0(X, \xi)$ arising from the parts $\mathcal{L}_1$, $\mathcal{L}_2$ and $\mathcal{C}$ of the contour sketched in figure 1 are identical to those relevant to the delta function shaped hump problem considered above.

Inclusion of the terms arising from poles in $\bar{F}(s)$ leads to the complete solution

$$v_0(X, \xi) = \left(\frac{9\lambda^{-\frac{1}{3}}}{2\pi i X^{\frac{5}{3}}}N(\eta) + \ldots\right) - \frac{3\lambda^{\frac{1}{3}}}{2i}M(X, \xi) \tag{2.11a}$$

as $X \to \infty$ where $N(\eta)$ is as defined in (2.6) and $M(X,\xi)$ satisfies

$$\frac{\partial^2 M}{\partial \xi^2} = -e^{iX+\frac{2i\pi}{3}}\,\mathrm{Ai}\left(\lambda^{\frac{1}{3}}e^{\frac{i\pi}{6}}\xi\right) + e^{-iX-\frac{2i\pi}{3}}\,\mathrm{Ai}\left(\lambda^{\frac{1}{3}}e^{-\frac{i\pi}{6}}\xi\right), \tag{2.11b}$$

with

$$M(X,0) = 0, \qquad \frac{\partial M}{\partial \xi}(X,0) = \frac{2i}{3\lambda^{\frac{1}{3}}}\cos X. \tag{2.11c}$$

Furthermore, if we denote the solution (2.8) of the delta function problem by $\hat{u}_0(X,\xi)$ then

$$\begin{aligned} u_0(X,\xi) = (\hat{u}_0(X,\xi) + \ldots) + \tfrac{3}{2}\lambda^{\frac{4}{3}}\left(Q_+(X,\xi) + Q_-(X,\xi)\right) \\ + \frac{1}{2i\,\mathrm{Ai}(0)}\left(\mathrm{Ai}(\lambda^{\frac{1}{3}}e^{\frac{i\pi}{6}}\xi)e^{iX} - \mathrm{Ai}(\lambda^{\frac{1}{3}}e^{-\frac{i\pi}{6}}\xi)e^{-iX}\right), \end{aligned} \tag{2.12a}$$

with

$$\begin{aligned} Q_\pm(X,\xi) = e^{\pm i(X+\frac{\pi}{6})}\Bigg\{ -\frac{\mathrm{Ai}(\lambda^{\frac{1}{3}}e^{\pm\frac{i\pi}{6}}\xi)}{3\,\mathrm{Ai}(0)\lambda^{\frac{4}{3}}}e^{\mp\frac{2i\pi}{3}} \\ -\frac{e^{\mp\frac{i\pi}{2}}}{\lambda}\int_\infty^\xi \mathrm{Ai}(\lambda^{\frac{1}{3}}e^{\pm\frac{i\pi}{6}}t)dt + \lambda^{-\frac{2}{3}}e^{\mp\frac{i\pi}{3}}\,\mathrm{Ai}'(0)\,\mathrm{Ai}(\lambda^{\frac{1}{3}}e^{\pm\frac{i\pi}{6}}\xi)\int_0^\xi \frac{\left(\int_\infty^u \mathrm{Ai}(\lambda^{\frac{1}{3}}e^{\pm\frac{i\pi}{6}}t)dt\right)}{\left\{\mathrm{Ai}(\lambda^{\frac{1}{3}}e^{\pm\frac{i\pi}{6}}u)\right\}^2}du\Bigg\}. \end{aligned} \tag{2.12b}$$

Although the periodic forcing (2.10) is very specific it does illustrate much of the nature of the Laplace transform solutions that arise from a wide variety of distributed functions. If the forcing has a zero mean value then $\bar{F}(s)$ tends to an O(1) constant as $s \to 0$ and so the $\mathcal{L}_1, \mathcal{L}_2$ and $\mathcal{C}$ parts of the contour for the Laplace inversion gives a solution proportional to (2.6a) for v_0 and (2.8) for u_0. On the other hand if $\bar{F}(s)$ has a simple pole at the origin (which corresponds to a distributed forcing function with non–zero mean) then we recover a multiple of the Heaviside type solution presented in §2.2. Each pole in $\bar{F}(s)$, other than at the origin $s = 0$, leads to terms like $M(X,\xi)$ in (2.11) and $Q_\pm(X,\xi)$ in (2.12a). These functions are periodic in X and for a general periodic forcing function these terms in the solutions for v_0 and u_0 need to be replaced by infinite sums akin to Fourier series.

The solutions (2.11a), (2.12a) indicate that as $X \to \infty$ the influence of the contributions arising from any poles of $\bar{F}(s)$ is confined to a thin region adjacent to the wall whereas those from the delta–function part of the solution expand into a region where $\xi = O(X^{\frac{1}{3}})$. Thus the solution parts divide into forms governed by two distinct structures and this point is explored further in the coming section.

3. The evolution of O(1) wavelength vortices further downstream

We now show how the solutions of the preceding section may be used to deduce unique initial conditions of a form suitable for the marching of equations (2.6a, b) to O(1) values of x. As we allow $X \to \infty$ the similarity variable implied by the results of §2 is

$$\zeta = y\,(\lambda/\tilde{x})^{\frac{1}{3}}, \qquad \tilde{x} = x - \bar{x}, \tag{3.1}$$

and for $\zeta = O(1)$ the appropriate expansions for the disturbance velocity components u and v are

$$u = \frac{\lambda^{\frac{1}{3}}}{\tilde{x}} u_0(\zeta) + \ldots, \qquad v = \frac{1}{\tilde{x}^{\frac{5}{3}}} v_0(\zeta) + \ldots, \tag{3.2a, b}$$

in the case of $F^*(X) = \delta(X)$. The functions u_0 and v_0 satisfy

$$\frac{d^2u_0}{d\zeta^2} + \tfrac{1}{3}\zeta^2 \frac{du_0}{d\zeta} + \zeta u_0 = v_0, \qquad \frac{d^4v_0}{d\zeta^4} + \tfrac{1}{3}\zeta^2 \frac{d^3v_0}{d\zeta^3} + \tfrac{7}{3}\zeta \frac{d^2v_0}{d\zeta^2} = 0, \tag{3.2c, d}$$

which need to be solved subject to

$$u_0 = v_0 = \frac{dv_0}{d\zeta} = 0, \quad \text{on} \quad \zeta = 0; \qquad u_0, \frac{dv_0}{d\zeta} \to 0 \quad \text{as} \quad \zeta \to \infty. \tag{3.3}$$

DHS observed that equation (3.2d) may be solved for $d^2v_0/d\zeta^2$ in terms of Whittaker functions. This equation is linear and the constant of proportionality in the solution comes directly from the Laplace solution (2.6a) so that

$$v_0 = \frac{9^{\frac{3}{4}}\lambda^{-\frac{1}{3}}}{2\pi} \int_0^{\zeta} \left\{ \int_0^{p} q^{-1} \exp\left(-\tfrac{1}{18}q^3\right) W_{2,\frac{1}{6}}\left(\tfrac{1}{9}q^3\right) dq \right\} dp. \tag{3.4}$$

Now DHS argued that the homogeneous form of equation (3.2c) has the eigensolution $u_{0H} = \zeta \exp\left(-\frac{1}{9}\zeta^3\right)$ and that any other linearly independent solution of (3.2c) behaves like $u_0 \sim \zeta^{-3}$ as $\zeta \to \infty$. In turn, since $u_{0H}(0) = 0$ it was stated that the inhomogeneous form of (3.2c) can only be solved if a finite multiple of the algebraically decaying solution is retained. In that case the solution cannot be matched with the flow in the core region where $y = O(1)$. It was therefore concluded that this similarity solution cannot be the required form for $\tilde{x}$ small. Instead, DHS proceeded to identify another similarity solution in which to leading order $u_0 \sim \tilde{x}^{-1}u_0(\zeta)$ and $v_0 \sim \tilde{x}^{-\frac{2}{3}}v_0(\zeta)$ and these forms of solutions led to the conclusion that the disturbance is confined to the region where $\zeta = O(1)$.

However the above argument is flawed as a particular solution of (3.2c) may be found which excludes the algebraically decaying homogeneous solution whilst at the same time vanishing at $\zeta = 0$. (That this is possible was kindly pointed out to us by Professor S.N. Brown.) Then

$$u_0 = D\zeta \exp(-\tfrac{1}{9}\zeta^3) - \tfrac{1}{6}\zeta v_0'' + \tfrac{1}{3}v_0' - \tfrac{5}{18}\zeta^2 v_0 + \zeta \exp(-\tfrac{1}{9}\zeta^3) \int_0^{\zeta} \left(\tfrac{7}{9} + \tfrac{5}{54}t^3\right) v_0(t) \exp(\tfrac{1}{9}t^3) dt, \tag{3.5}$$

is a suitable solution of (3.2a) where D is some constant whose value is as yet unknown. Its value could be determined by examining further terms in the similarity expansions (3.2a, b) but it is much more convenient to deduce the required value directly from the Laplace transform solution (2.7). This gives

$$D = \frac{1}{2\sqrt{3}\pi}\left(7\,\mathrm{Ai}(0) + \frac{3\,\mathrm{Ai}'(0)}{\mathrm{Ai}(0)}\right)\Gamma(\tfrac{4}{3}). \tag{3.6}$$

Solutions (3.4–6) describe how the vortex develops at small O(1) distances downstream of a delta-shaped hump and within $O(\tilde{x}^{\frac{1}{3}})$ distances of the wall. They therefore provide suitable starting conditions for a numerical solution of equations (2.6a, b) to greater distances downstream.

For the case $F^*(X) = H(X)$ the Laplace solutions (2.9a, c) suggest that for $0 < \tilde{x} \ll 1$

$$u = u_0(\zeta) + \ldots, \qquad v = \tilde{x}^{-\frac{2}{3}} v_0(\zeta) + \ldots, \tag{3.7}$$

with

$$\frac{d^2u_0}{d\zeta^2} + \tfrac{1}{3}\zeta^2\frac{du_0}{d\zeta} = v_0, \qquad \frac{d^4v_0}{d\zeta^4} + \tfrac{1}{3}\zeta^2\frac{d^3v_0}{d\zeta^3} + \tfrac{4}{3}\zeta\frac{d^2v_0}{d\zeta^2} = 0. \tag{3.8}$$

Now

$$v_0 = -\frac{3\sqrt{3}\lambda^{-\frac{1}{3}}}{2\pi}\int_0^\zeta \left(\frac{\zeta}{t} - 1\right)\exp(-\tfrac{1}{18}t^3)W_{1,\frac{1}{6}}(\tfrac{1}{9}t^3)dt, \tag{3.9}$$

in order to match with solution (2.9c). There is a subtle difference in the solution of the u_0 equation (3.8a) in contrast to that of equation (3.2a). In the latter case it was seen that of the two homogeneous solutions of the equation one decays algebraically whilst the other decays exponentially and also vanishes at $\zeta = 0$. Hence the unknown D was contained in solution (3.5) and needed to be deduced by using extra information. However (3.8a) has the homogeneous solutions $u_0 = 1$ and $u_0 = \int_0^\zeta \exp(-\frac{1}{9}t^3)dt$ so this equation has a unique solution when the boundary conditions $u_0(0) = 1$, $u_0 \to 0$ as $\zeta \to \infty$ are imposed (with the first condition coming from (1.6e)). Thence

$$u_0 = A\int_\infty^\zeta \exp(-\tfrac{1}{9}t^3)dt + \int_\infty^\zeta \exp(-\tfrac{1}{9}t^3)\left\{\int_0^t v_0(q)\exp(\tfrac{1}{9}q^3)dq\right\}dt, \tag{3.10}$$

where the constant A is chosen so that $u_0(0) = 1$.

In the two cases described above we have derived solutions of equations (1.6a, b) valid for $0 < \tilde{x} \ll 1$ and $y = O(\tilde{x}^{\frac{1}{3}})$. To deduce the requisite forms for $y = O(1)$ we let the similarity variable $\zeta \to \infty$ and then

$$u = \frac{\lambda^{\frac{1}{3}}\bar{u}'}{\tilde{x}^\beta\bar{u}}q^*(y,k) + \ldots, \qquad v = \frac{1}{\tilde{x}^{1+\beta}}q^*(y,k) + \ldots, \tag{3.11}$$

where the function $q^*(y,k)$ has been defined by (2.4) and the constant $\beta = \frac{2}{3}$ for $F^*(X) = \delta(X)$ and $\beta = -\frac{1}{3}$ for the Heaviside forcing. In this way we have solutions

valid for small distances downstream of the roughness element and these may be used to initiate the numerical solutions of (2.6a, b).

Finally we discuss the case of the distributed roughness element. As before we shall concentrate on the particular case $F(X) = \sin X$ where $X = \tilde{x}/\varepsilon$ although the analysis is easily extended to other functions. The solution for $\tilde{x} \ll 1$ is composed of two parts. The first of these is just the delta–function solution given in §3.1 above whereas the second contains the fast streamwise variation arising from the form of the forcing function. Then where the similarity variable $\zeta = O(1)$ the solutions for u and v develop according to

$$u \sim \left(\frac{\lambda^{\frac{1}{3}}\varepsilon}{\tilde{x}} u_0(\zeta) + \ldots\right) + \left(\left(\frac{\varepsilon\lambda}{\tilde{x}}\right)^{\frac{1}{3}} \hat{U}_0(X,\zeta) + \ldots\right), \tag{3.12a}$$

$$v \sim \left(\frac{\varepsilon}{\tilde{x}^{\frac{5}{3}}} v_0(\zeta) + \ldots\right) + \left(\varepsilon^{-\frac{2}{3}} \hat{V}_0(X,\zeta) + \ldots\right), \tag{3.12b}$$

where u_0, v_0 are as given in (3.2–4) and

$$\zeta \frac{\partial \hat{U}_0}{\partial X} + \hat{V}_0 = 0, \qquad \frac{\partial^2}{\partial \zeta^2}\left(\frac{\partial \hat{V}_0}{\partial X}\right) = 0. \tag{3.13}$$

These equations cannot be solved subject to the necessary conditions that $\hat{U}_0 = F(X) = \sin X$ and $\hat{V}_0 = 0$ on $y = 0$. Then in an inner layer where $Y = y/\varepsilon^{\frac{1}{3}} = O(1)$ the 'fast' part of the solution (3.12) develops as

$$u \sim \ldots\ldots + U_0^{\dagger}(X,Y), \qquad v \sim \ldots\ldots + \varepsilon^{-\frac{2}{3}} V_0^{\dagger}(X,Y), \tag{3.14}$$

with

$$V_0^{\dagger} = P_+ e^{iX} + P_- e^{-iX}, \tag{3.15a}$$

$$P_{\pm} = \frac{3\lambda^{\frac{1}{3}}}{2}\left[-e^{\pm\frac{i\pi}{6}} Y \int_Y^{\infty} \mathrm{Ai}(\lambda^{\frac{1}{3}} e^{\pm\frac{i\pi}{6}} t)dt - \lambda^{-\frac{2}{3}} e^{\mp\frac{i\pi}{6}}\left(\mathrm{Ai}'(\lambda^{\frac{1}{3}} e^{\pm\frac{i\pi}{6}} Y) - \mathrm{Ai}'(0)\right)\right] \tag{3.15b}$$

and

$$\lambda Y \frac{\partial U_0^{\dagger}}{\partial X} + \lambda V_0^{\dagger} = \frac{\partial^2 U_0^{\dagger}}{\partial Y^2}, \tag{3.15c}$$

subject to $U_0^{\dagger}(X,0) = \sin X$ and $U_0^{\dagger} \to 0$ as $Y \to \infty$. It is straightforward to verify that as $Y \to \infty$ so

$$V_0^{\dagger} \to 3\lambda^{-\frac{1}{3}} \mathrm{Ai}'(0)\cos(X - \tfrac{1}{6}\pi) \quad \text{and} \quad U_0^{\dagger} \to 3\lambda^{-\frac{1}{3}} \mathrm{Ai}'(0)\cos(X + \tfrac{1}{3}\pi)/\zeta, \tag{3.16}$$

which shows that the functions $\hat{U}_0(X,\zeta)$ and $\hat{V}_0(X,\zeta)$ defined in (3.12) are given by

$$\hat{U}_0 = \frac{3\lambda^{-\frac{1}{3}} \mathrm{Ai}'(0)}{\zeta}\cos(X + \tfrac{1}{3}\pi), \qquad \hat{V}_0 = 3\lambda^{-\frac{1}{3}} \mathrm{Ai}'(0)\cos(X - \tfrac{1}{6}\pi). \tag{3.17}$$

Finally we have that in the $y = O(1)$ region the 'slow' and 'fast' parts of the solution develop according to

$$u \sim \frac{\varepsilon\lambda^{\frac{1}{3}}\bar{u}'}{\tilde{x}^{\frac{1}{3}}}q^*(y,k) + \ldots\ldots + \varepsilon^{\frac{1}{3}}\hat{\hat{U}}_0(X,y) + \ldots\ldots,$$
$$v \sim \frac{1}{\tilde{x}^{\frac{5}{3}}}q^*(y,k) + \ldots\ldots + \varepsilon^{-\frac{2}{3}}\hat{\hat{V}}_0(X,y) + \ldots\ldots, \tag{3.18}$$

where

$$\hat{\hat{V}}_0 = 3\lambda^{-\frac{1}{3}}\,\mathrm{Ai}'(0)q^*(y,k)\cos(X - \tfrac{1}{6}\pi), \qquad \hat{\hat{U}}_0 = 3\lambda^{-\frac{1}{3}}\bar{u}'\,\mathrm{Ai}'(0)q^*(y,k)\cos(X + \tfrac{1}{3}\pi)/\bar{u}$$

and $q^*(y,k)$ has been defined by the Rayleigh equation (2.4).

We consequently have the result that for the distributed forcing problem the solution structure in the vicinity of the start of the forcing is composed of three distinct regions. The component of the solution associated with the fast streamwise variation satisfies the Rayleigh equation for $y = O(1)$, is given by the simple pair of equations (3.13) when $\zeta = O(1)$ and is governed by viscous-type balances where $y = O(\varepsilon^{\frac{1}{3}})$. This structure contrasts to that relevant to the isolated forcing case in which this last region adjacent to $y = 0$ is not required.

For O(1) values of x we can seek a solution of (1.6) corresponding to a distributed wall roughness with non–zero mean value. If $y = O(1)$ then

$$u = u_S(x,y) + \varepsilon^{\frac{1}{3}}u_F(x,X,y) + \cdots,$$
$$v = v_S(x,y) + \varepsilon^{-\frac{2}{3}}v_F(x,X,y) + \cdots, \tag{3.19}$$

where the fast functions u_F and v_F are periodic in X with zero mean and are, at leading order in ε, proportional to $q^*(y,k)$. If the expansions (3.19) are substituted into (1.6) and we average with respect to the fast variable X we see that u_S and v_S also satisfy (1.6). We note here the fact that u_F and v_F are driven directly by the wall forcing and adjust to the forcing in wall layers of thickness $O(\varepsilon^{\frac{1}{3}})$. Moreover, we stress that the fact that the Görtler number is O(1) means that no growth or decay of the vortex is possible on the short $O(\varepsilon)$ scale so we monitor the evolution of the vortex just in terms of u_S and v_S. Since the small $\tilde{x}$ forms of these functions are given by the leading order terms in (3.18a,b) it follows that the stability problem for the $F^*(X) = \sin X$ forcing is, at leading order in ε, identical to that for the delta function case. In a similar way, for distributed periodic functions which provoke the small slow x response appropriate to a Heaviside function the stability problem defined in terms of the slow response of the vortex is identical to that for the case $F^*(X) = H(X)$. It follows that, so long as we define instability in terms of the appropriate downstream scale, i.e. $x = O(1)$, we can use results from the cases $F^*(X) = \delta(X)$ and $H(X)$ in order to deduce the stability properties of Görtler vortices induced by a general wall forcing shape.

4. The numerical work

The similarity solutions derived in the preceding section yield the unique vortex forms valid at small distances downstream of the forcing function. In order to investigate the development of vortices at O(1) downstream distances it is necessary to solve equations $(1.6a, b)$ numerically. Since these equations are parabolic in nature a standard marching scheme was implemented in order to follow the flow from $x = \frac{1}{2} + \Delta x$ where Δx is a small specified distance from the start of the forcing. The details of the numerical technique closely follow those given by Hall (1983) and the reader is referred to that article for a full description. Certain modifications were found to be required for the current problem– in particular equations $(1.6a, b)$ were finite–differenced in y but in order to resolve the initial vortex form which is concentrated close to $y = 0$ it was necessary to replace the uniform grid employed by Hall (1983) by a variable spaced mesh with nodes tightly packed near $y = 0$ but relatively sparsely spaced as $y \to \infty$.

The solutions presented in this paper were all verified by making the usual checks that the results were independent of grid spacing and choice of Δx. As a measure of the disturbance energy we monitored the value of

$$E = \int_0^\infty (u^2 + v^2 + w^2) dy,$$

and defined the local growth rate $\beta = E^{-1} dE/dx$. The position of neutral stability can be taken to be the location at which $\beta = 0$ and this position does depend to some extent on the choice of the particular flow property used to define β. (This point is discussed in detail by Hall (1990).)

For a selection of values of k with fixed values of G we calculated the position at which the induced vortex structure begins to grow. The local wavenumber k_x and local Görtler number G_x were evaluated at that point and used to generate a neutral curve in the (k_x, G_x) plane. It is worthwhile to emphasise that since the forcing was applied at the same point $(x = \frac{1}{2})$ for each calculation, the Görtler number G is a measure of how close the forcing is to the unstable region.

We first report on the calculations for the delta–function forcing considered in §2.1. In this case the leading order similarity solution valid a small distance downstream of the forcing at $x = \frac{1}{2}$ is given by $(3.2a, b)$, (3.4)–(3.6), (3.11) and these were used to initiate the computations at $x = \frac{1}{2} + \Delta x$. However we found that these leading order solutions are insufficiently accurate for our purposes for when these were used our computed neutral curves were not independent of grid spacing or the choice of Δx. Therefore it was deemed necessary to develop a further term in the similarity solution (3.2). This is a routine task and it was found that these two leading terms in the small $(x - \frac{1}{2})$ solutions were sufficient to ensure adequate convergence.

Our results for the delta–function problem are summarised in Figure 2 where we show neutral curves for a variety of values of G. We observe that the lowest critical Görtler number occurs when G is about 8 and then takes a value of about 15.5. This is somewhat greater than that found by DHS (who quoted a lowest critical value of 12) whose computations were started with the incorrect similarity forms. This therefore suggests that localised wall roughness in its most dangerous form produces growth in the vortex structure when the local Görtler number is roughly 15.5. In Figure 3 we give further details of the envelope of the neutral curves of Figure 2. We see in Figure 3 that initially G_c decreases with G up to the point where $G \approx 8$ after which G_c increases with G. The critical wavenumber k_c is a monotonic decreasing function of G and at the lowest critical G_c, $k_c \approx 0.92$.

In Figure 2 we have also indicated the asymptotic form of the neutral stability curve which is valid for large k_c. This asymptotic expression may be deduced from the workings of Hall (1982) and we see that the first two terms of this asymptotic expansion gives surprisingly good agreement with our computed values even at quite modest values of k_c.

We turn now to study the problem of Heaviside forcing as developed in §2.2. In this case we again initiated our calculations using the first two terms in the requisite similarity solution forms in order to achieve satisfactory convergence. The dependences of critical Görtler number G_c and local vortex wavenumber k_c are shown as functions of G in Figure 4. We note the radically different behaviours of these forms when compared with the results for the isolated delta–function forcing problem. In particular we note that both k_c and G_c are monotonic functions of G and, in particular, $G_c \to 0$ as $G \to 0$. This means that the critical Görtler number can be reduced to an arbitrarily small value by choosing the origin where the forcing begins increasingly close to the leading edge. Thus it appears that when the forcing commences near the leading edge only a very small amount of wall curvature is required in order to cause vortex growth.

As was pointed out in the preceding section we may deduce the vortex response due to a general distributed wall forcing by examining the stability characteristics of the Görtler modes for the delta– function and Heaviside wall problems. When the forcing function has zero mean value then the appropriate stability characteristics close to the start of the forcing are reminiscent of the results for the delta–function case whereas for a non–zero mean valued wall forcing it is the results summarised in figure 4 which are pertinent.

5. Conclusion

In this work we have described how isolated and distributed roughness elements can stimulate the growth of linearised Görtler vortices. In particular, Laplace transform techniques are required in order to deduce how vortex modes evolve close to the forcing. Integration of the full governing equations allows the development of vortices to be

monitored at O(1) distances downstream of the commencement of the forcing. This numerical integration requires suitable initial vortex profiles to be specified and these (necessarily unique) forms may be found in the form of similarity solutions which may be derived directly from the Laplace solutions. Two specific forcing functions have been considered in our work. First, a delta–function was taken as a model of an isolated roughness element and the stability characteristics of induced vortices computed. This calculation was previously performed by DHS but faulty initial conditions meant that their conclusions regarding the receptivity of O(1) wavelength vortices were unreliable. Our improved workings have led us to conclude that isolated elements can trigger unstable vortices at local Görtler number greater than about 15.5 but for G_x less than this value the flow is not susceptible to vortex instabilities.

When the isolated element is replaced by a distributed roughness patch we have shown that the stability characteristics of induced modes are radically altered. Of importance, we have seen that as the Görtler number decreases to zero so the critical local wavenumber k_c grows and the critical local Görtler number $G_c \to 0$. This suggests that distributed wall forcing can be extremely important in generating Görtler modes since irrespective of the particular value of G_x unstable modes can exist. As was pointed out by DHS, for free–stream disturbances the critical G_c is roughly 6 so that free–stream disturbances are clearly less dangerous in provoking Görtler vortices than are distributed wall elements. However these free–stream disturbances are more significant than isolated roughnesses and, for a general roughness profile composed of both distributed and short–scale variations we have shown that it is the former type which tends to dictate the receptivity properties of the flow. DHS suggested that the localised wall roughness mechanism would be relevant only in an experimental facility with remarkably tiny free–stream disturbances. Our work here allows us to extend this conclusion and speculate that a distributed wall element provides the easiest route to the generation of vortex modes.

Unfortunately there are few experiments carried out on the Görtler vortex problem; in fact we are unaware of any experiments which address the receptivity problem for Görtler vortices. The fundamental experimental difficulty with the problem is that results appear not to be reproducible from day to day with the same apparatus. It is likely that this is caused by the sensitive dependence on initial conditions which the vortices exhibit, see Hall (1983) for an explanation of why this is the case. However if wall roughness is sufficiently large then it is probable that it will lead directly to the linear growth of vortices, the analysis we have given here can then be used to predict the response of the flow. Note here that it is a simple matter to extend the analysis to describe three-dimensional objects, see DHS, so that controlled experiments could be carried out in order to see the response of

the flow to different wall disturbances. Thus we argue that the present calculation gives the experimentalist, for the first time, a chance to obtain agreement between theory and experiment in the Görtler problem.

References

Abramowitz, M. and Stegun, I.A. 1965 *Handbook of Mathematical Functions.* Dover, New York.

Denier, J.P., Hall, P. and Seddougui, S.O. 1991 On the receptivity problem for Görtler vortices– vortex motions induced by wall roughness. *Phil. Trans. R. Soc. Lond. A.* **335**, 51-85.

Hall, P. 1982 Taylor–Görtler vortices in fully developed or boundary layer flows: linear theory. *J. Fluid Mech.* **124**, 475–494.

Hall, P. 1983 The linear development of Görtler vortices in growing boundary layers. *J. Fluid Mech.* **130**, 41–58.

Hall, P. 1990 Görtler vortices in growing boundary layers: the leading edge receptivity problem, linear growth and the nonlinear breakdown stage. *Mathematika* **37**, 151–189.

Hall, P. and Morris, H. 1992 On the instability of boundary–layers on heated flat plates. *J. Fluid Mech.* **245**, 367–400.

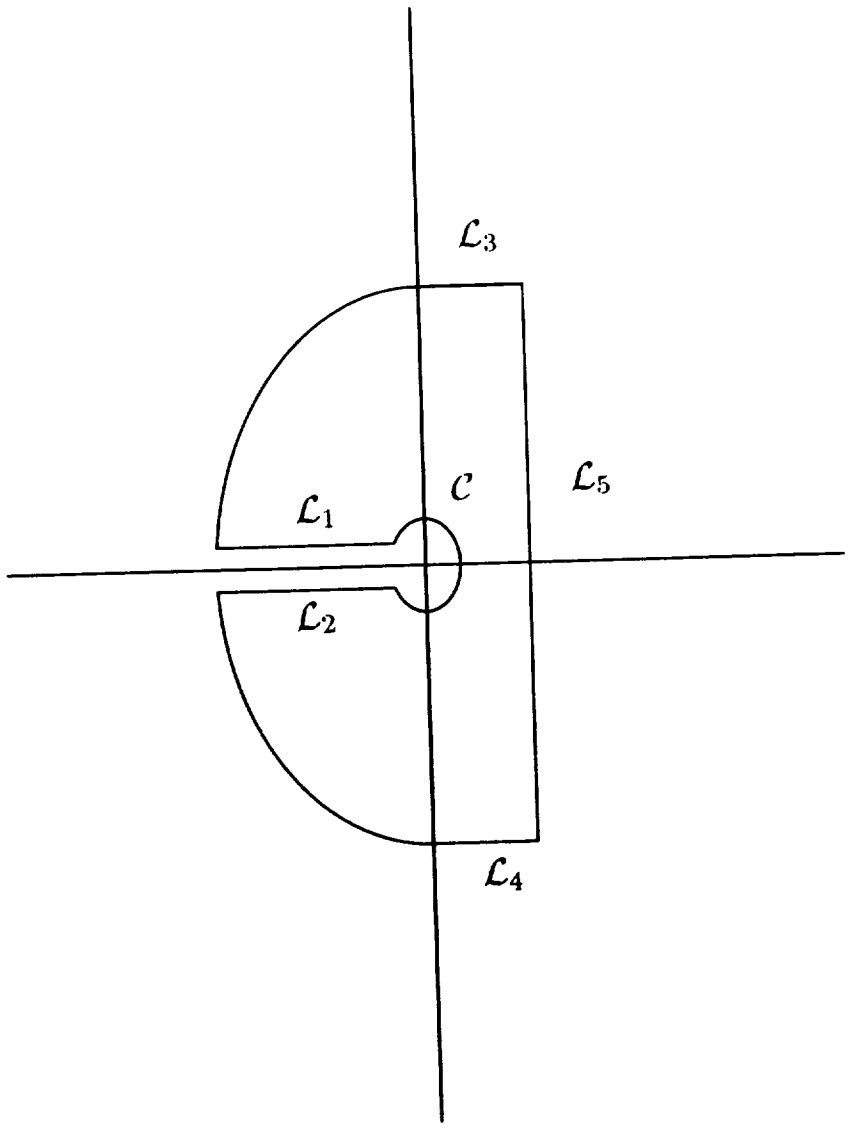

Figure 1. The key-hole contour used to evaluate the Laplace inversions of §2. The complex s-plane is cut along the negative real axis and the contour consists of two large arcs of radii R, linear portions lines $\mathcal{L}_1$, $\mathcal{L}_2$, $\mathcal{L}_3$, $\mathcal{L}_4$ and $\mathcal{L}_5$as shown. The line $\mathcal{L}_1$ and $\mathcal{L}_2$ are located above and below the branch cut and a small circle C of radius δ. Integrals along the line parallel to the imaginary axis passing through the point $s = c + 0i$ may be deduced by allowing $R \to \infty$, $\delta \to 0$ and then applying Cauchy's residue theorem.

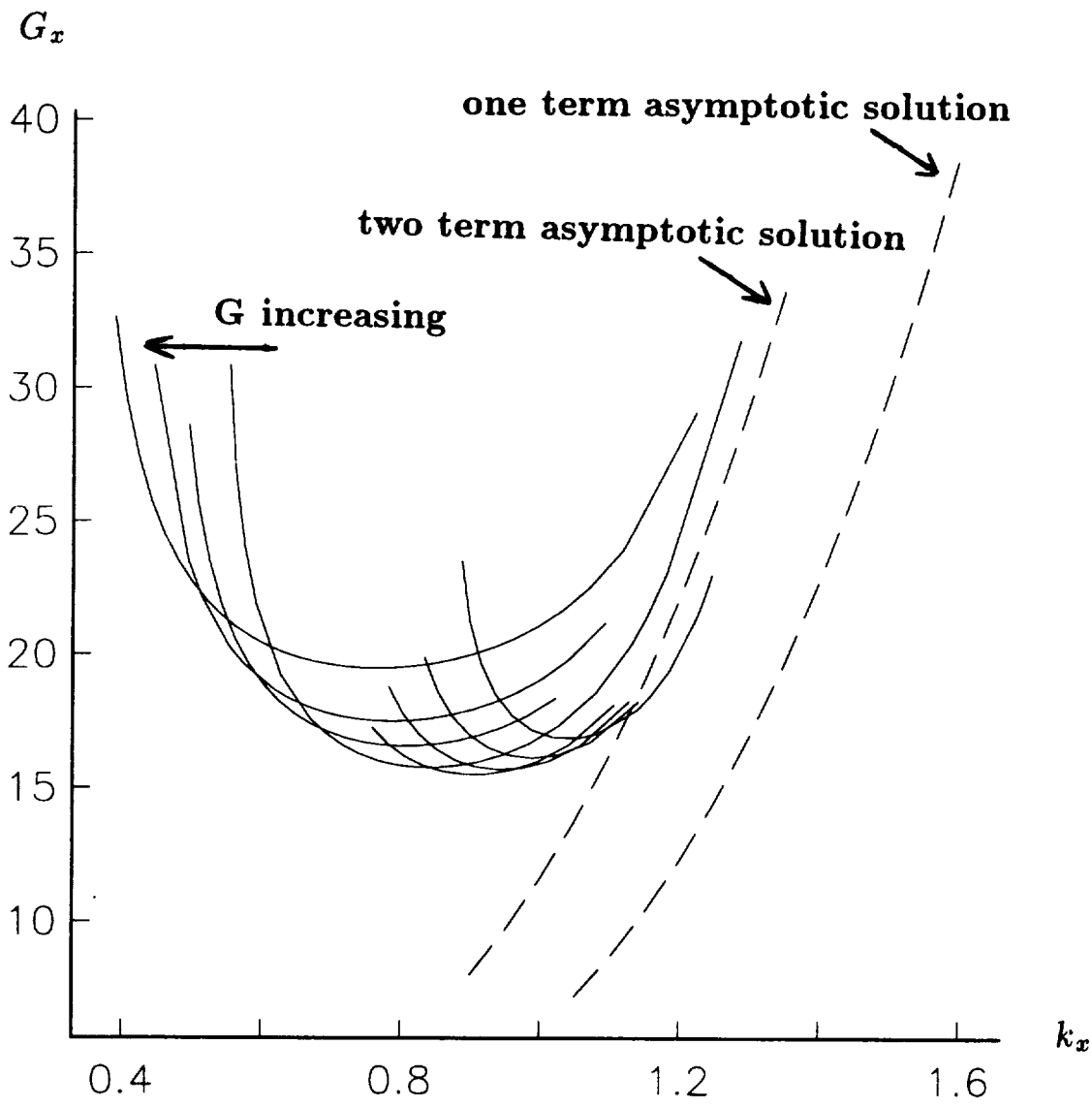

Figure 2. The neutral curves corresponding to a delta–function shaped wall forcing and an initial disturbance constructed from the first two terms of the similarity solution which starts as in (3.2). The curves correspond to the values $G = 5., 5.7, 6.5, 7.5, 10., 12.5, 15., 20.$ The dashed curves are the one term and two term forms of the appropriate large wavenumber right–hand neutral branch (derived from Hall 1982).

Figure 3. The critical local Görtler number G_c as a function of the Görtler number G appropriate to a delta–function wall forcing.

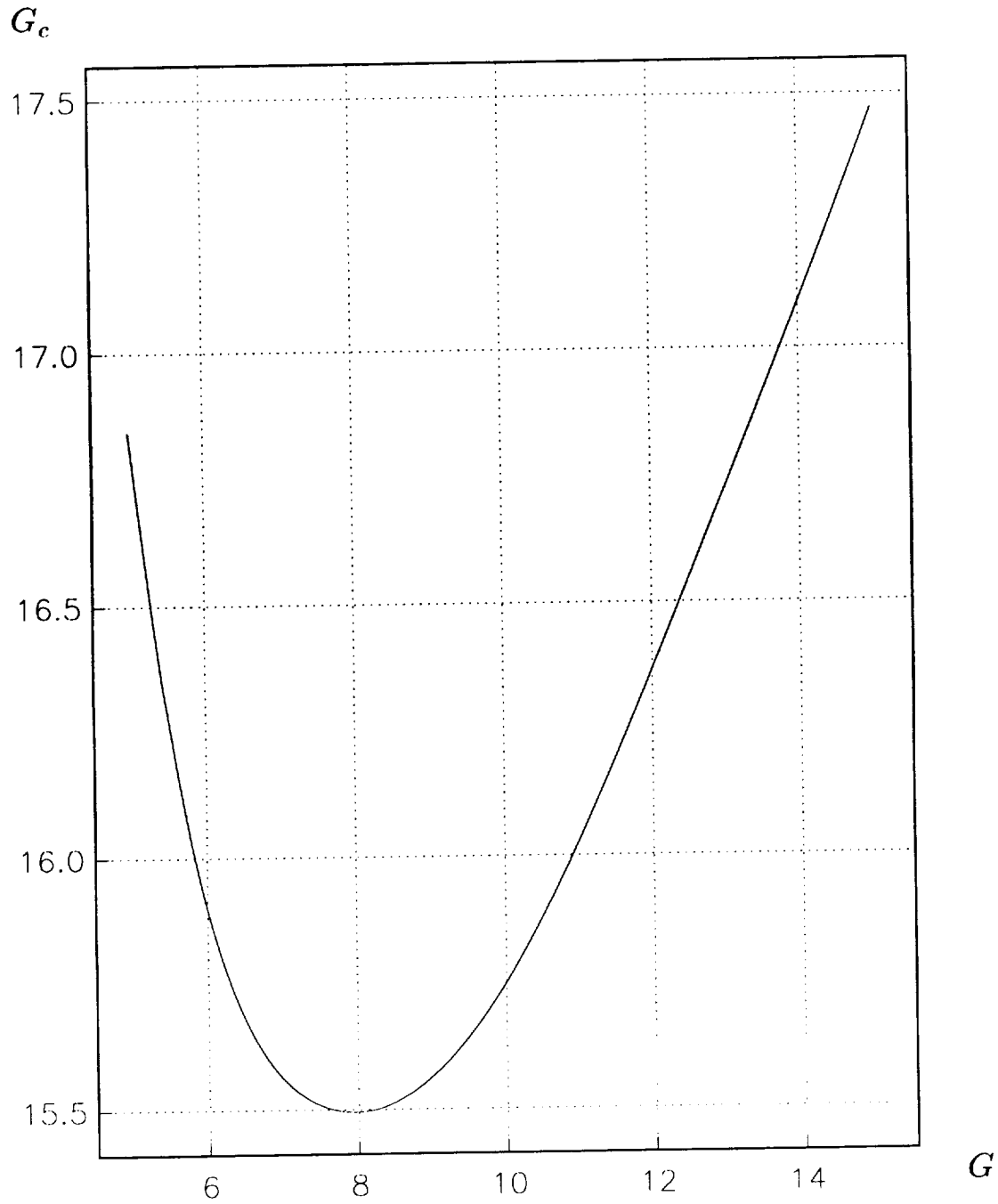

Figure 4. *a)* The critical local Görtler number G_c and *b)* the critical local vortex wavenumber k_c as functions of the Görtler number G appropriate to a Heaviside–function wall forcing.

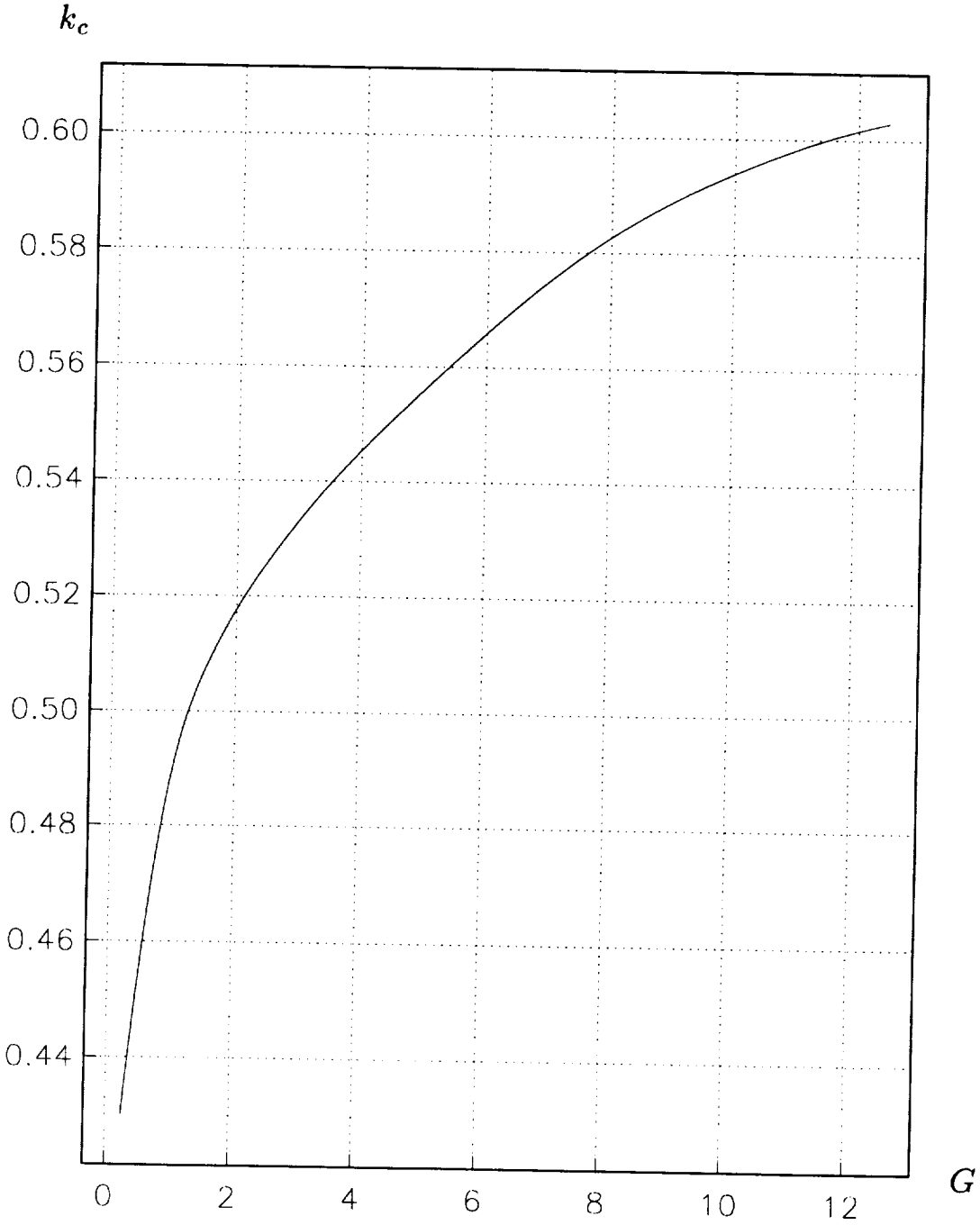

Figure 4. *a)* The critical local Görtler number G_c and *b)* the critical local vortex wavenumber k_c as functions of the Görtler number G appropriate to a Heaviside–function wall forcing.

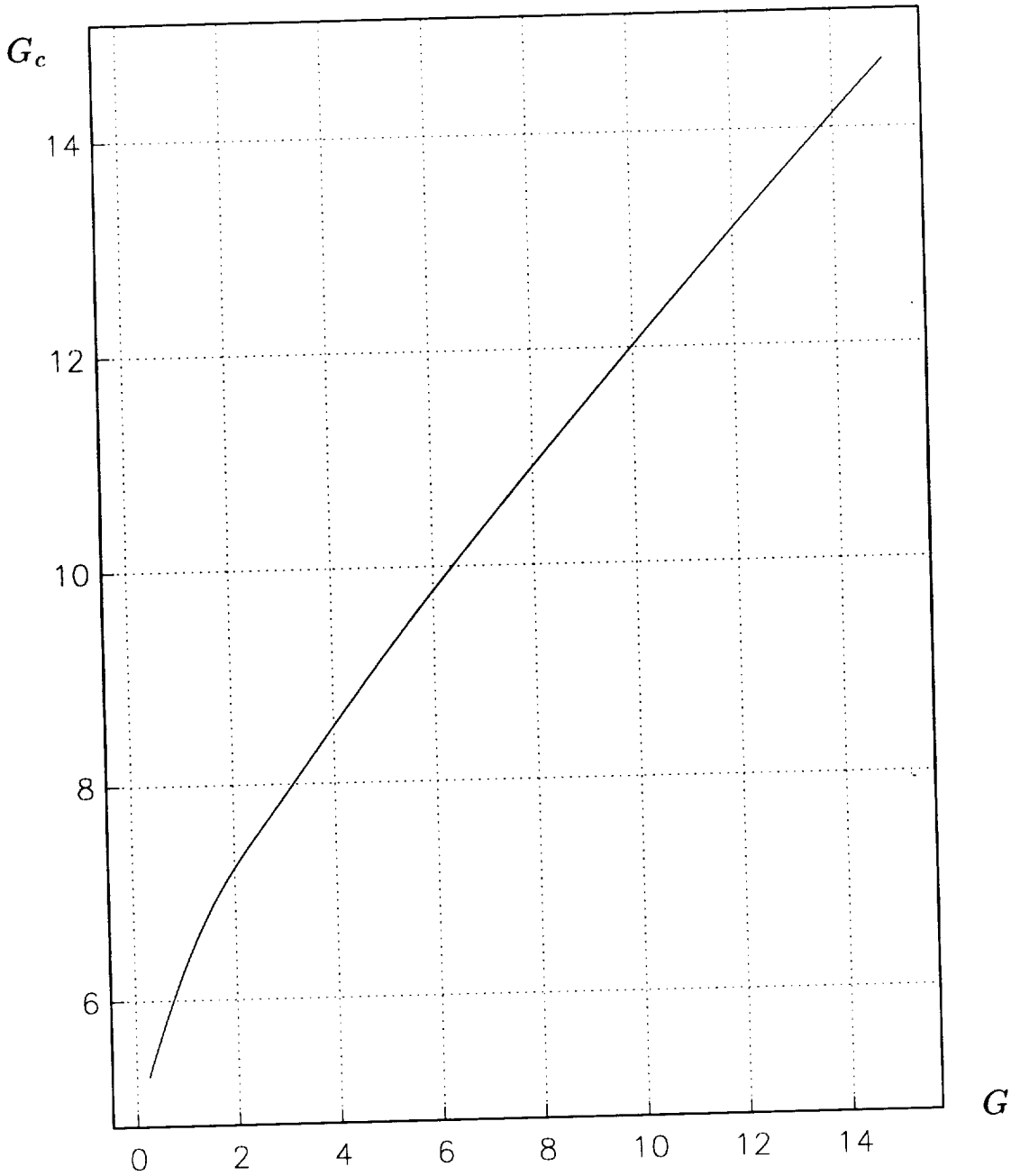

REPORT DOCUMENTATION PAGE

Form Approved
OMB No. 0704-0188

1. AGENCY USE ONLY (Leave blank)	2. REPORT DATE	3. REPORT TYPE AND DATES COVERED
	August 1993	Contractor Report

4. TITLE AND SUBTITLE

ON THE RECEPTIVITY PROBLEM FOR O(1) WAVELENGTH GÖRTLER VORTICES

5. FUNDING NUMBERS

C NAS1-19480

WU 505-90-52-01

6. AUTHOR(S)

Andrew P. Bassom
Philip Hall

7. PERFORMING ORGANIZATION NAME(S) AND ADDRESS(ES)

Institute for Computer Applications in Science and Engineering
Mail Stop 132C, NASA Langley Research Center
Hampton, VA 23681-0001

8. PERFORMING ORGANIZATION REPORT NUMBER

ICASE Report No. 93-58

9. SPONSORING/MONITORING AGENCY NAME(S) AND ADDRESS(ES)

National Aeronautics and Space Administration
Langley Research Center
Hampton, VA 23681-0001

10. SPONSORING/MONITORING AGENCY REPORT NUMBER

NASA CR-191519
ICASE Report No. 93-58

11. SUPPLEMENTARY NOTES

Langley Technical Monitor: Michael F. Card
Final Report

Submitted to Proc. Roy. Soc. London A

12a. DISTRIBUTION/AVAILABILITY STATEMENT

Unclassified - Unlimited

Subject Category 34

12b. DISTRIBUTION CODE

13. ABSTRACT (Maximum 200 words)

In this paper we make an investigation of the receptivity of boundary layer flows to Görtler vortex modes. A study by Denier, Hall, and Seddougui (1991) of the generation of vortices by wall roughness elements concluded that such elements are extremely poor as mechanisms to stimulate short wavelength modes but that analysis was in error. We re-examine this problem here and demonstrate how the form of the wall roughness is crucial in determining the vortex stability characteristics downstream of the roughness. In particular we investigate the cases of both isolated and distributed forcing functions and show that in general a distributed function is much more important in generating vortices than are either isolated roughness or free-stream disturbances.

14. SUBJECT TERMS

receptivity, vortex

15. NUMBER OF PAGES

25

16. PRICE CODE

A03

17. SECURITY CLASSIFICATION OF REPORT	18. SECURITY CLASSIFICATION OF THIS PAGE	19. SECURITY CLASSIFICATION OF ABSTRACT	20. LIMITATION OF ABSTRACT
Unclassified	Unclassified		

NSN 7540-01-280-5500

Standard Form 298 (Rev. 2-89)
Prescribed by ANSI Std. Z39-18
298-102

☆U.S. GOVERNMENT PRINTING OFFICE: 1993 - 728-064/86053